Supplementary Information

Amirhossein Mirtaleb and Ruigang Wang*
Department of Chemical Engineering and Materials Science,
Michigan State University, East Lansing, MI 48824
rwang@msu.edu

Figure S1. Photographic Appearance of Composite Electrolyte Membranes

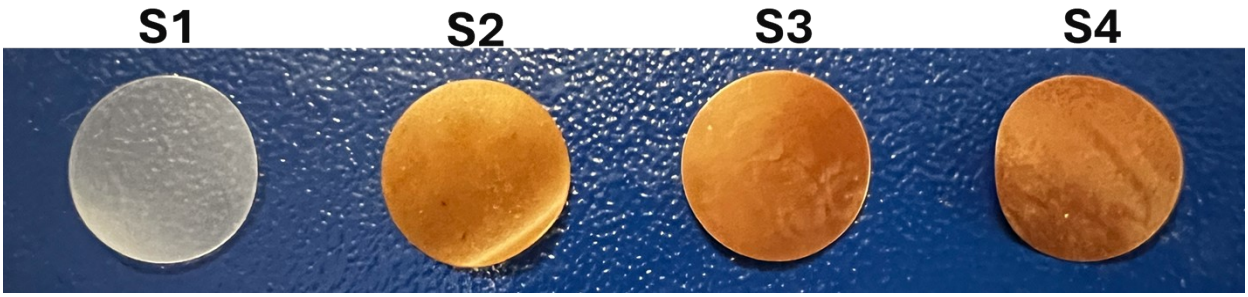

Figure S1: Photographs of PVDF–LiTFSI–$Li_7P_{2.9}Ce_{0.1}S_{11}$ composite polymer electrolyte films with increasing ceramic filler content (0, 5, 10, and 15 wt%, left to right).

Table S1. Composite Electrolyte Composition

The precise formulation of the PVDF–LiTFSI–$Li_7P_{2.9}Ce_{0.1}S_{11}$ composite polymer electrolytes is given in Table S1.

Table S1: Composition of PVDF–LiTFSI–$Li_7P_{2.9}Ce_{0.1}S_{11}$ composite polymer electrolyte samples with varying filler loadings, showing $Li_7P_{2.9}Ce_{0.1}S_{11}$, PVDF, and LiTFSI masses (mg) and total solid mass.

Sample	Filler Content (wt%)	$Li_7P_{2.9}Ce_{0.1}S_{11}$ (mg)	PVDF (mg)	LiTFSI (mg)	Total Solids (mg)
S1	0%	0	880	400	1280
S2	5%	64	816	400	1280
S3	10%	128	752	400	1280
S4	15%	192	688	400	1280

Figure S2. Synthesis procedures for assembling coin cells

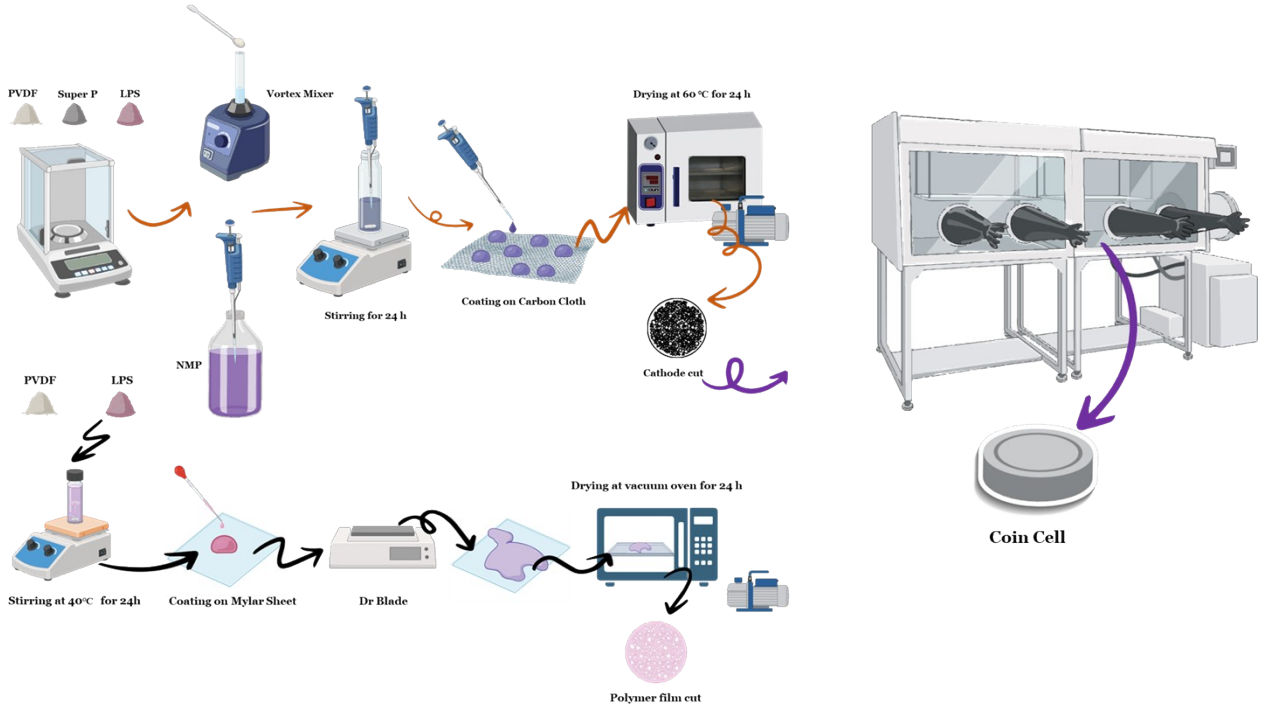

Figure S2: Schematic diagram: synthesis procedures for assembling coin cells with composite polymer electrolyte.

Figure S3. Morphology and Elemental Distribution of the Neat Polymer Electrolyte (PE)

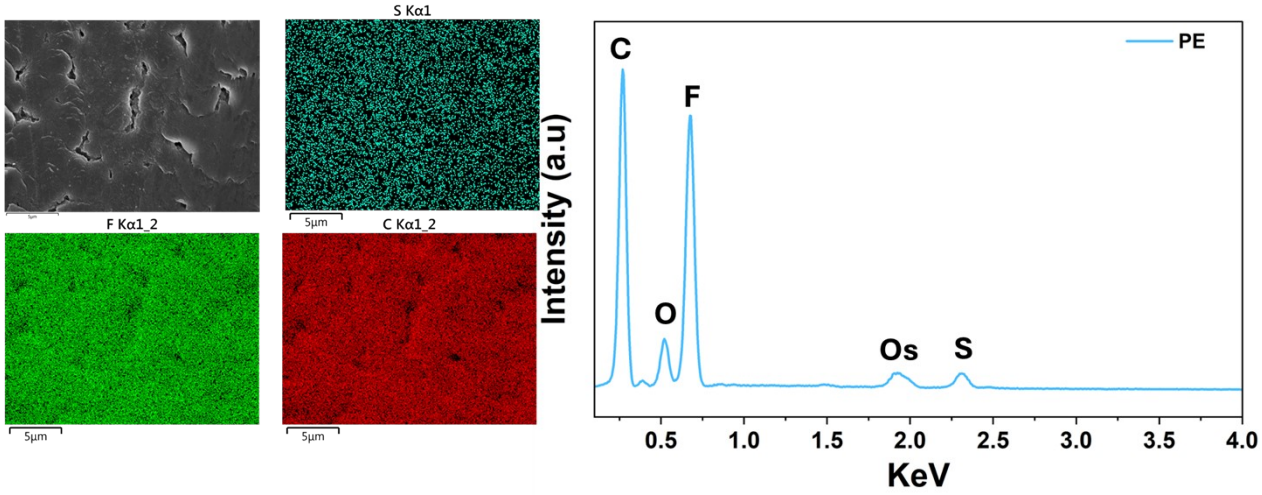

Figure S3: SEM, elemental mapping, and EDS spectrum of the neat polymer electrolyte (PE), showing uniform C, F, and O distribution with trace S and Os from PVDF–LiTFSI and osmium coating.

Figure S4. Morphology and Elemental Distribution of the 10 wt% $Li_7P_{2.9}Ce_{0.1}S_{11}$ Composite Polymer Electrolyte (CPE)

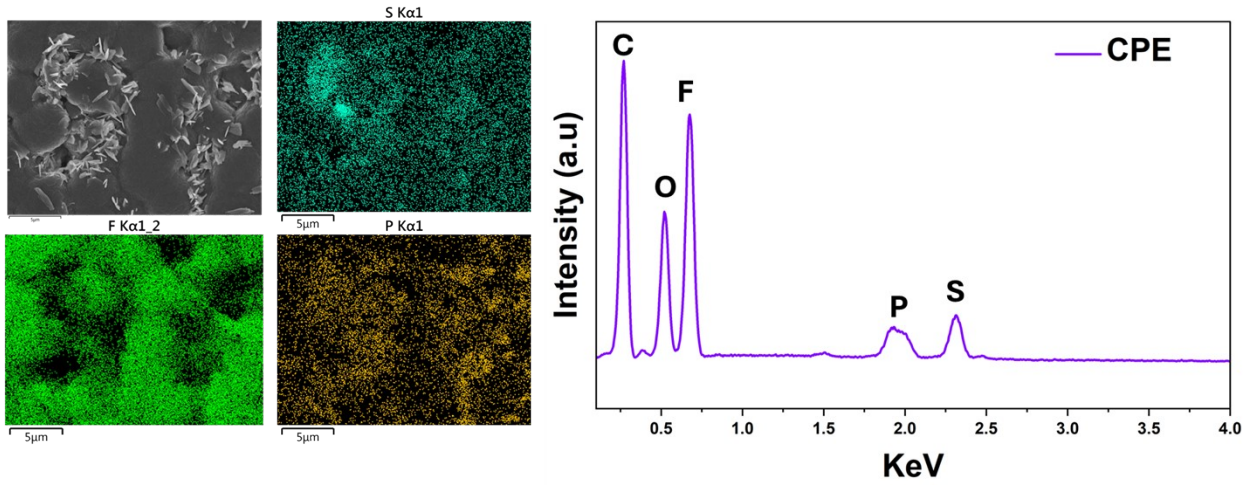

Figure S4: SEM, elemental mapping, and EDS spectrum of the CPE with 10 wt% $Li_7P_{2.9}Ce_{0.1}S_{11}$, showing uniformly distributed ceramic fillers and confirming the presence of C, F, O, P, and S.

Table S2. Li^+ Transference Number Calculation

The Li^+ transference number (t_+) was determined using the Bruce–Vincent method, which combines chronoamperometry and electrochemical impedance spectroscopy (EIS). A symmetric Li — electrolyte — Li cell was polarized under a constant DC voltage of ΔV = 50 mV, and the current response was recorded from the initial current I_0 to the steady-state current I_{ss}. The interfacial plus bulk resistances before and after polarization (R_0 and R_{ss}) were extracted from Nyquist plots collected immediately before and after the DC step.

The transference number was calculated using the Bruce–Vincent equation:

$$t_+^{Li+} = \frac{I_{ss}\cdot(\Delta V - I_0 R_0)}{I_0\cdot(\Delta V - I_{ss} R_{ss})}$$

The calculated values are summarized in Table S2.

Table S2: Parameters and calculated Li^+ transference numbers for PE and CPE cells under a 50 mV DC bias.

Electrolyte	R_0 (Ω)	R_{ss} (Ω)	I_0 (A)	I_{ss} (A)	t_+
PE (no filler)	80.9	93.0	3.90×10^{-4}	2.295×10^{-4}	0.375
CPE (with filler)	20.4	21.0	1.16×10^{-4}	7.348×10^{-5}	0.623

Table S3. Benchmarking of Electrochemical Performance in Solid-State Li–S Batteries

Table S3: Comparison of electrochemical performance of various solid-state and composite polymer electrolyte (CPE)-based Li–S battery systems.

System	Electrolyte Type	Ionic Conductivity ($S \cdot cm^{-1}$)	S Loading ($mg \cdot cm^{-2}$)	Initial Capacity ($mAh \cdot g^{-1}$)	1000-cycle Capacity ($mAh \cdot g^{-1}$)	Retention (%)	t_+	Window (V)	Reference
This work	PVDF–LiTFSI + 10 wt% $Li_7P_{2.9}Ce_{0.1}S_{11}$	9.0×10^{-4}	1.0 / 5.0	1610 @ 0.2C	642 @ 1C	~ 39	0.6	~4.5	This work
Wu et al., 2020	LLZO–PVDF–HFP	~ 1.2×10^{-4}	2.0	1245 @ 0.2C	680 @ 300 cyc	~55	~0.3	~4.5	[1]
Yu & Manthiram, 2021	PEO–LLZO composite	~ 5.0×10^{-5}	2.5	~1350 @ 0.1C	700 @ 300 cyc	~52	0.2–0.3	~4.2	[2]
Liu et al., 2016	PAN gel polymer	1.0×10^{-3}	1.5	~1500 @ 0.1C	~800 @ 200 cyc	~53	–	~4.6	[3]
Wei et al., 2023	$MoTe_2$@Graphene CPE	~ 6.4×10^{-4}	1.2	1583 @ 0.2C	890 @ 500 cyc	~ 56	–	~4.3	[4]
Pan et al., 2022	In_2S_3-doped $Li_7P_3S_{11}$	3.1×10^{-3}	2.0	1492 @ 0.2C	1100 @ 200 cyc	~74	–	~ 5	[5]
Zhang et al., 2016	Garnet–PEO	4.2×10^{-5}	1.0	1150 @ 0.1C	600 @ 100 cyc	~52	~0.25	~4.6	[6]

References

[1] M. Wu, D. Liu, D. Qu, Z. Xie, J. Li, J. Lei, and H. Tang. 3d coral-like llzo/pvdf composite electrolytes with enhanced ionic conductivity and mechanical flexibility for solid-state lithium batteries. *ACS Applied Materials Interfaces*, 12(47):52652–52659, 2020.

[2] X. Yu and A. Manthiram. A review of composite polymer–ceramic electrolytes for lithium batteries. *Energy Storage Materials*, 34:282–300, 2021.

[3] M. Liu, D. Zhou, Y.-B. He, Y. Fu, X. Qin, C. Miao, H. Du, B. Li, Q.-H. Yang, and Z. Lin. Novel gel polymer electrolyte for high-performance lithium–sulfur batteries. *Nano Energy*, 22:278–289, 2016.

[4] Y. Wei, B. Zhao, C. Song, J. Wu, W. Wu, and L. Yao. Flexible composite polymer electrolyte based on $mote_2$@graphene for high-performance lithium-sulfur batteries. *Journal of Colloid and Interface Science*, 635:391–400, 2023.

[5] H. Pan, Y. Liu, Z. Liu, X. Chen, Y. Zhang, and L. Wang. All-solid-state lithium–sulfur batteries enabled by in_2s_3-doped $li_7p_3s_{11}$ solid electrolyte. *ACS Applied Energy Materials*, 5(11):13429–13438, 2022.

[6] J. Zhang, N. Zhao, M. Zhang, Y. Li, P. K. Chu, X. Guo, Z. Di, X. Wang, and H. Li. Flexible and ion-conducting membrane electrolytes for solid-state lithium batteries: dispersion of garnet nanoparticles in insulating polyethylene oxide. *Nano Energy*, 28:447–454, 2016.